

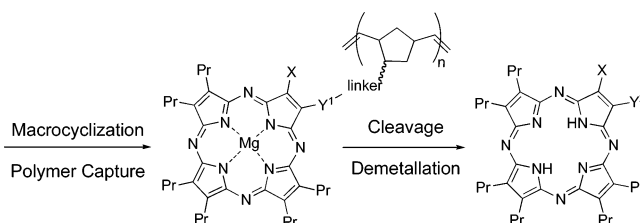
ROM Polymerization-Capture-Release Strategy for the Chromatography-Free Synthesis of Novel Unsymmetrical Porphyrazines

Matthew J. Fuchter,[†] Benjamin J. Vesper,[‡] Karen A. Murphy,[†] Hazel A. Collins,[†]
David Phillips,[†] Anthony G. M. Barrett,^{*,†} and Brian M. Hoffman^{*,‡}

Department of Chemistry, Imperial College London, London SW7 2AZ, U.K., and Department of
Chemistry, Northwestern University, Evanston, Illinois 60208

agmb@imperial.ac.uk; bmh@northwestern.edu

Received December 17, 2004



Crossover-Linstead macrocyclization reactions of two norbornenyl-tagged diaminomaleonitriles with dipropylmaleonitrile gave access to crude mixtures of porphyrazines containing diamino-hexapropylporphyrazine magnesium complexes. The mixtures were subjected to ring-opening metathesis polymerization to yield the insoluble diaminoporphyrazine-functionalized polymers. Acid-mediated cleavage from the polymer backbone followed by acylation of the resultant sensitive macrocyclic diamines gave monoacetyl-, monotrifluoroacetyl-, and ditrifluoroacetyl-substituted porphyrazine-diamines. Conversion of these amido-porphyrazines to the corresponding zinc macrocycles and studies of their electronic absorption and emission spectra, electrochemistry, and photophysics are described.

Introduction

Porphyrazines are structural variants of porphyrins, with meso nitrogen atoms replacing the meso carbon atoms. Although the related porphyrins and phthalocyanines have received considerable interest and detailed studies into their synthesis, properties, and applications have been reported,^{1,2} porphyrazines have received significantly less attention. Peripheral heteroatom functionalization of the macrocycle results in significant modulation of their physical and electronic properties.³ Barrett, Hoffman, and co-workers have published extensively on the synthesis of porphyrazines bearing thiols, amines, or alcohols as ring substituents and with the conversion of these polydentate ligands to a variety of coordination complexes.^{3,4} Since its development in 1952,

the Linstead macrocyclization⁵ of acyclic maleonitriles is still the only widely used method for porphyrazine synthesis. Although it is hard to picture a faster or more versatile route, the procedure is frequently plagued with poor yields and difficulties with purification. In addition, the selective synthesis of specific constitutional isomers from the crossover macrocyclization of two different maleonitriles (respectively functionalized by A and B) is limited. For phthalocyanines, methods to achieve direct synthesis of specific isomers include the linking of two phthalonitrile units prior to macrocyclization,^{6,7} ring expansion of a subphthalocyanine,^{8,9} solid-phase synthesis,^{10,11} and the preparation of “half-phthalocyanine” intermediates.¹² For porphyrazines, the employment of

[†] Imperial College London.

[‡] Northwestern University.

(1) *The Porphyrins*; Dolphin, D., Ed.; Academic Press: New York, 1978–1979; Vol. 1–7.

(2) *Phthalocyanines: Properties and Applications*; Leznoff, C. C., Lever, A. B. P., Eds.; VCH Publishers: Weinheim, Germany, 1989–1996; Vol. 1–4.

(3) Stuzhin, P. A.; Ercolani, C. In *The Porphyrin Handbook*; Kadish, K. M., Smith, K. M., Guillard, R., Eds.; Academic Press: New York, 2003; Vol. 15, p 263.

(4) Michel, S. L.; Baum, S.; Barrett, A. G. M.; Hoffman, B. M. In *Progress in Inorganic Chemistry*; Karlin, K. D., Ed.; Wiley & Sons: New York, 2001; Vol. 50, p 473.

(5) Linstead, R. P.; Whalley, M. *J. Chem. Soc.* **1952**, 4839.

(6) Kobayashi, N.; Kobayashi, Y.; Osa, T. *J. Am. Chem. Soc.* **1993**, *115*, 10994.

(7) Drew, D. M.; Leznoff, C. C. *Synlett* **1994**, 623.

(8) Kobayashi, N.; Kondo, R.; Nakajima, S.-I.; Osa, T. *J. Am. Chem. Soc.* **1990**, *112*, 9640.

(9) Kobayashi, N.; Ishizaki, T.; Ishii, K.; Konami, H. *J. Am. Chem. Soc.* **1999**, *121*, 9096.

(10) Leznoff, C. C.; Hall, T. W. *Tetrahedron Lett.* **1982**, *23*, 3023.

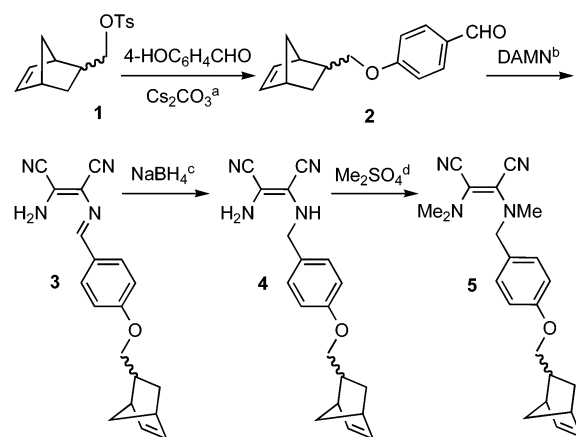
dinitriles bearing bulky groups (trans directors) to give *trans*-A₂B₂ porphyrazines selectively has been demonstrated.¹³ Statistical cyclization of two maleonitrile components, resulting in a mixture of constitutional isomers, is currently the only viable method for the synthesis of unsymmetrical porphyrazines (A₃B). Drawing on experience in ring-opening metathesis (ROM) polymerization¹⁴ and impurity annihilation,¹⁵ we sought to improve the synthetic strategy for elaborating polyfunctional porphyrazines. Hanson and co-workers have recently demonstrated the application of chemically tagged reagents for the synthesis of *o*-alkylhydroxylamines, amines, and alkyl hydrazines.^{16,17} The principle of employing a norbornenyl-tagged reagent, with solution-phase Linstead macrocyclization and subsequent selective capture of the desired porphyrazine by ROM polymerization, is appealing. Cleavage of the macrocycle from the ROM polymer should deliver the pure porphyrazine without the need for extensive chromatography. Ruthenium alkene metathesis catalysts, developed by Grubbs,^{18,19} have been previously applied to the synthesis of polymeric porphyrazine structures²⁰ and therefore should be ideal for this application.

Results and Discussion

Norbornenyl-tagged dinitrile **5** was prepared in four steps from diaminomaleonitrile and known tosylate **1**,²¹ which was converted into aldehyde **2** by reaction with cesium carbonate and 4-hydroxybenzaldehyde. Following the procedure of Sheppard and co-workers,²² condensation of aldehyde **2** and diaminomaleonitrile gave imine **3**, which was subsequently reduced with sodium borohydride. Resultant maleonitrile **4**, which was obtained in 70% yield over two steps, was used directly without further purification. Methylation using dimethyl sulfate and sodium hydride gave tagged aminomaleonitrile **5** in 93% yield (Scheme 1).

Macrocyclization of aminomaleonitrile **5** and dipropylmaleonitrile **6** (9.9 equiv)²³ gave a crude mixture of dyes containing porphyrazines **7** and **8**, as identified by FAB mass spectrometry (Scheme 2). Unfortunately, treatment of this mixture with Grubbs' second-generation catalyst **10**^{18,19} and cross-linker **11** under standard ROM polymerization conditions¹⁴ gave no polymeric products. This was initially attributed to the presence of excess mag-

SCHEME 1



Reagents and conditions:

- (a) 4-HOC₆H₄CHO, Cs₂CO₃, DMF, Δ, 16 h, 96 %;
 (b) H₂N(CN)C=C(CN)NH₂, EtOH, Δ, 20 h, 73 %;
 (c) NaBH₄, MeOH, THF, 2 h, 96 %; (d) Me₂SO₄, NaH, THF, -30 °C to 20 °C, 18 h, 93 %.

nesium butoxide used in the cyclization, which destroyed the active catalyst. However, all attempts to neutralize the residual base prior to polymerization using stoichiometric quantities of acetic acid, acid-washed Celite, carboxylic acid-functionalized Amberlyst resin, or silica gel failed to facilitate polymerization. Finally, rapid filtration of the crude mixture through silica followed by evaporation of the filtrate and reaction of the residue with catalyst **10** resulted in the formation of ROM polymer **9** as an insoluble blue solid.

Treatment of ROM polymer **9** with TFA in dichloromethane resulted in the simultaneous cleavage of the linker and demetalation of the supported porphyrazine to give the expected macrocycle **12** (Scheme 2). Under optimum conditions, addition of a 10% solution of TFA in dichloromethane to ROM polymer **9** followed by stirring at ambient temperature for 1 h gave porphyrazine **12** (17% overall from **5**) after filtration through silica. This yield is comparable to structurally similar free-base porphyrazine **13**, which was obtained after chromatography in 19% yield.²⁴ The analogous yields imply that the lowest yielding step is the macrocyclization reaction, with both polymerization and cleavage presumably occurring efficiently. Porphyrazine **12** proved to be unstable, even when stored under argon at -18 °C. This was presumably due to the increased electron donation of the free amino functionality into the ring system, leading to an electron-rich macrocycle prone to oxidative degradation. It was therefore not straightforward to determine the purity of porphyrazine **12**, and only limited characterization was achieved. However, porphyrazine **12** was successfully converted into other more robust derivatives. Attempted methylation using methyl iodide at reflux or dimethyl sulfate at room temperature under basic conditions, central metalation of porphyrazine **12** using zinc acetate, or peripheral metalation using palladium(II) chloride or (PhCN)₂PtCl₂²⁴ resulted only in

(11) Hirth, A.; Sobbi, A. K.; Wöhrle, D. *J. Porphyrins Phthalocyanines* **1997**, *1*, 275.

(12) Nolan, K. J. M.; Hu, M.; Leznoff, C. C. *Synlett* **1997**, 593.

(13) Forsyth, T. P.; Williams, D. B. G.; Montalban, A. G.; Stern, C. L.; Barrett, A. G. M.; Hoffman, B. M. *J. Org. Chem.* **1998**, *63*, 331.

(14) Barrett, A. G. M.; Hopkins, B. T.; Köbberling, J. *Chem. Rev.* **2002**, *102*, 3301.

(15) Barrett, A. G. M.; Smith, M. L.; Zecri, F. *Chem. Commun.* **1998**, 2317.

(16) Harned, A. M.; Hanson, P. R. *Org. Lett.* **2002**, *4*, 1007.

(17) Mukherjee, S.; Poon, K. W. C.; Flynn, D. L.; Hanson, P. R. *Tetrahedron Lett.* **2003**, *44*, 7187.

(18) Trnka, T. M.; Grubbs, R. H. *Acc. Chem. Res.* **2001**, *34*, 18.

(19) Bielawski, C. W.; Grubbs, R. H. *Angew. Chem., Int. Ed.* **2000**, *39*, 2903.

(20) Montalban, A. G.; Steinke, J. H. G.; Anderson, M. E.; Barrett, A. G. M.; Hoffman, B. M. *Tetrahedron Lett.* **1999**, *40*, 8151.

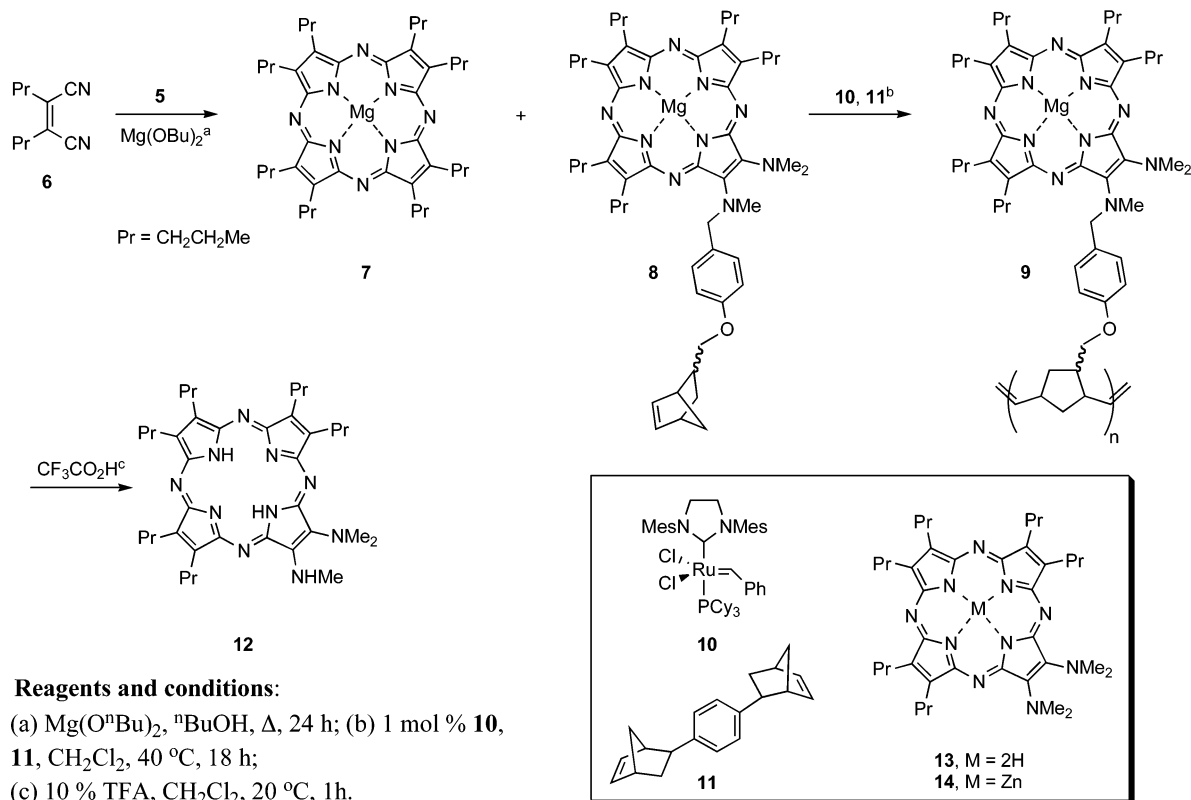
(21) Billet, E. H.; Fleming, I.; Hanson, S. W. *J. Chem. Soc., Perkin Trans.* **1973**, *1*, 1661.

(22) Begland, R. W.; Hartter, D. R.; Jones, F. N.; Sam, D. J.; Sheppard, W. A.; Webster, O. W.; Weigert, F. J. *J. Org. Chem.* **1974**, *39*, 2341.

(23) Fitzgerald, J.; Taylor, W.; Owen, H. *Synthesis* **1991**, 686.

(24) Lange, S. J.; Nie, H.; Stern, C. L.; Barrett, A. G. M.; Hoffman, B. M. *Inorg. Chem.* **1998**, *37*, 6435.

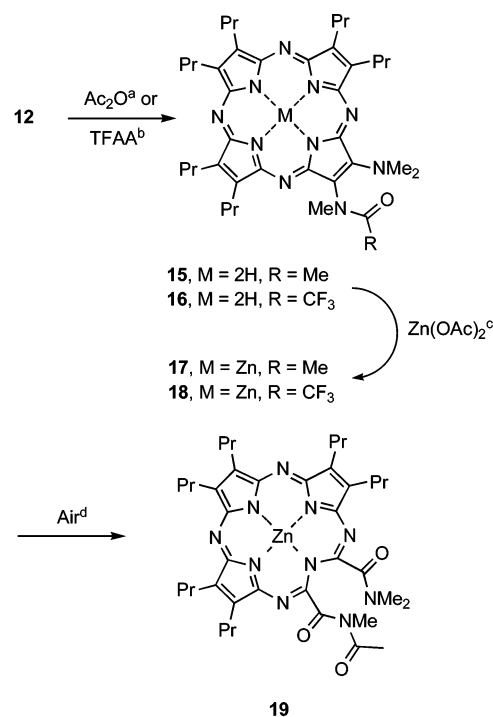
SCHEME 2



decomposition. The reaction of porphyrazine **12** with benzoyl or acetyl chloride and zinc acetate in pyridine at reflux, a solvent known to hinder oxidative degradation,²⁵ was examined in an attempt to both metalate the macrocycle and acylate the free amino group. Both reactions gave amide **15** as the sole product. Presumably, with benzoyl chloride, this arose from the formation of benzoic acetic anhydride. When optimized, reflux of macrocycle **12** and acetic anhydride in degassed pyridine gave amide **15** (95%). Similarly, acylation of porphyrazine **12** with trifluoroacetic anhydride in pyridine at 0 °C gave trifluoroacetamide **16** (65%) (Scheme 3).

In a modified procedure, porphyrazine **12** was allowed to react with either acetic anhydride or trifluoroacetic anhydride, with ScavengePore phenethyl piperidine added to remove excess anhydride. The solvent was evaporated under reduced pressure, and the product was filtered through silica to remove decomposition products. In the case of trifluoroacetylated product **15**, an additional aqueous workup was employed to remove residual salts, which could not be precipitated out of solution, prior to filtration. This gave porphyrazines **15** and **16** in >99 and 93% purity, respectively, as judged by HPLC. Porphyrazines **15** and **16** were readily converted to their zinc derivatives (**17** and **18**) using standard methods (Scheme 3). Interestingly, the NMR spectra of zinc porphyrazines **17** and **18** had to be recorded in pyridine-*d*₅ to avoid severe broadening of the peaks. As noted for the *sec*-oporphyrazines,²⁵ this can be attributed to the formation of dimer pairs via coordination of the amido oxygen atoms

SCHEME 3

**Reagents and conditions:**

(a) Ac₂O, py, Δ, 18 h, 95 %; (b) TFAA, py, 0 °C, 0.5 h, 65 %; (c) Zn(OAc)₂, DMF, 80 °C, 16 h; (d) CH₂Cl₂, air, 20 °C, 8 d, 86 %.

(25) Montalban, A. G.; Lange, S. J.; Beall, L. S.; Mani, N. S.; Williams, D. J.; White, A. J. P.; Barrett, A. G. M.; Hoffman, B. M. *J. Org. Chem.* **1997**, *62*, 9284.

to the apical site of the square-pyramidal zinc(II) center of the adjacent macrocycle.

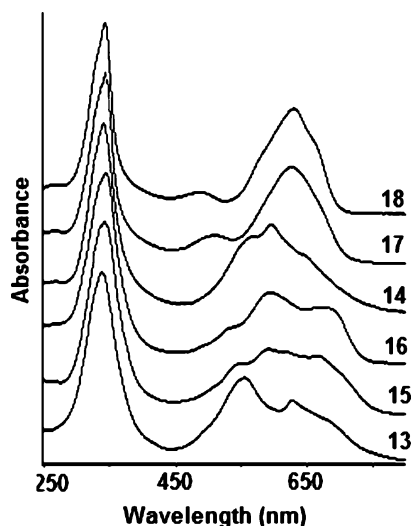


FIGURE 1. UV-vis spectra for porphyrazines **13**–**18** in $\text{CH}_2\text{-Cl}_2$.

The electronic absorption spectra of porphyrazines **13**–**18** are shown in Figure 1. Free-base porphyrazines **15** and **16** exhibit complex red-shifted Q bands in comparison to previously reported free-base A_3B porphyrazine **13**.²⁵ The spectra contain qualitatively similar absorbances at 342, 549, 591, and 668 nm and 344, 540, 595, and 670 nm, respectively. The broadened, complex Q band is a result of the reduced symmetry of the macrocycles in accordance with Gouterman's four-orbital model²⁶ as well as the electronic decoupling of one of the peripheral nitrogen lone pairs from the macrocyclic core by the electron-withdrawing acetyl or trifluoroacetyl groups. In addition, underlying $n-\pi^*$ transitions of the remaining lone pairs into a π^* ring orbital complicate the spectra.⁴ The broadened transition for metalated A_3B porphyrazine **14**²⁵ conceals the split of the Q band that is expected for the lower (C_{2v}) symmetry.²⁶ Once again, macrocycles **17** and **18** display spectra with qualitatively similar absorbances at 342, 508, and 626 nm and 342, 490, and 630 nm, respectively, which are red-shifted compared to those of structurally similar porphyrazine **14**. As with the free-base porphyrazines, substitution of the electronically deactivating acetyl and trifluoroacetyl groups results in desymmetrization of the π chromophore and subsequent disruption of the Q band transitions. Representative absorption and emission spectra of zinc porphyrazines **17** and **18** are shown in Figure 2.

The significant donation of electron density from the peripheral amino groups into the macrocyclic ring system has been previously demonstrated by cyclic voltammetry.⁴ Consequently, these porphyrazines are more easily oxidized than the analogous phthalocyanines and porphyrins. However, substitution of an electronically withdrawing acetyl or trifluoroacetyl group should result in an increase in the oxidation potential of the resulting porphyrazines, which leads to a macrocycle that is more difficult to oxidize. Indeed, the first oxidation potentials of **15** and **17** are 0.135 and 0.138 V, respectively, indicating that the macrocycles are at least 265 mV more

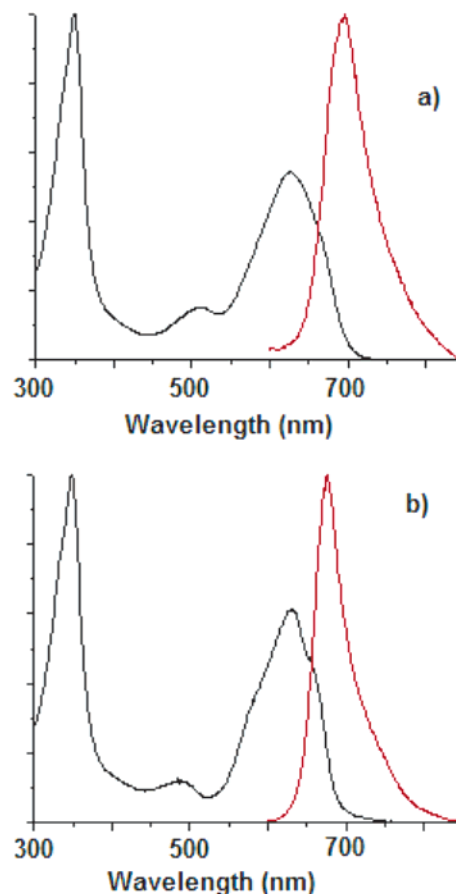


FIGURE 2. Absorption and emission spectra of (a) **17** and (b) **18** in toluene, $\lambda_{\text{ex}} = 511$ and 485, respectively.

difficult to oxidize than **13** (Figure 3, Table 1). Additionally, trifluoroacetyl-functionalized porphyrazines **16** and **18** exhibit first oxidation potentials at 0.287 and 0.306 V, respectively, demonstrating that the macrocycles are at least 417 mV more difficult to oxidize than **13** (Table 1). Free-base porphyrazines **15** and **16** also exhibit two reversible ring-based reductions at -1.57 , -1.99 and -1.476 , -1.89 V, respectively (Table 1). Although metalation with the redox-inactive zinc appears not to influence the macrocycle-based ring properties greatly, the second reduction potentials for porphyrazines **17** and **18** are shifted to potentials more negative than the window of the experiment following metalation.

The increased oxidation potential of porphyrazine **17** is reflected in the chemical oxidation to corresponding *seco*-porphyrazine **19** (Scheme 3). Treatment of porphyrazine **17** with potassium permanganate in dichloromethane for 3 h resulted in only trace amounts of *seco* derivative **19**. Previously, macrocycle **14** was converted to the corresponding *seco*-porphyrazine in almost quantitative yield using analogous conditions.²⁵ Alternatively, aerobic oxidation could be affected by stirring a dichloromethane solution containing **17** for a total of 8 days, periodically isolating small quantities of *seco* derivative **19**.

The electronic absorption spectrum of *seco* derivative **19** exhibits the characteristic split Soret and Q bands that are observed for the *seco*-porphyrazines, with absorbances at 341, 357, 572, and 651 nm, whereas the emission spectrum ($\lambda_{\text{ex}} = 566$ nm) displays a maxima at

(26) Gouterman, M. In *The Porphyrins*; Dolphin, D., Ed.; Academic Press: New York, 1978; Vol. 3, p 1.

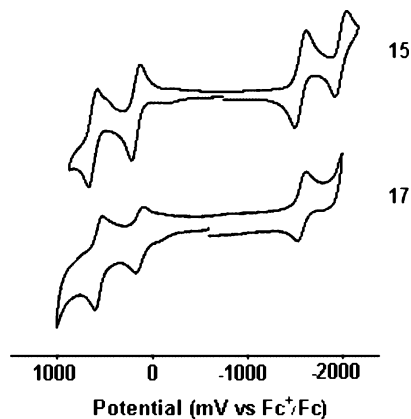


FIGURE 3. Cyclic voltammograms of porphyrazines **15** and **17**.

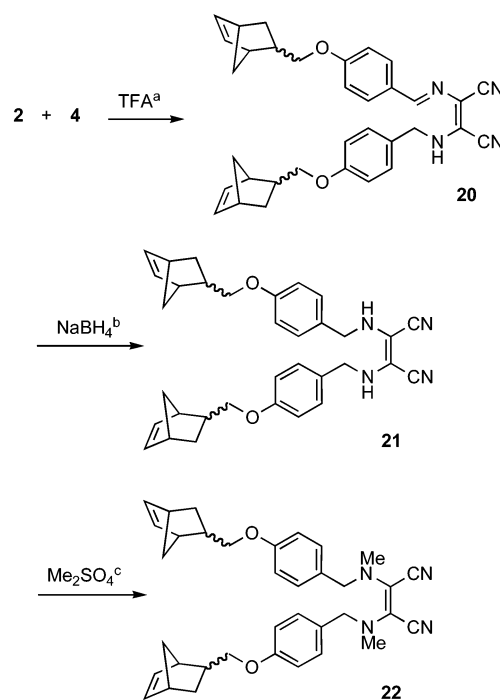
TABLE 1. Electrochemical Study of Porphyrazines 15–18

	comparison of half-wave potentials (V vs Fc ⁺ /Fc ⁰ , E _{1/2} (ΔE _p , mV)			
	pz ²⁺ /pz ⁺	pz ⁺ /pz	pz/pz ¹⁻	pz ¹⁻ /pz ²⁻
13 ⁴	+0.43(66)	-0.13(70)	-1.39(76)	-1.84(94)
15	+0.584(88)	+0.135(86)	-1.570(116)	-1.99(120)
16	+0.781(82)	+0.287(86)	-1.476(128)	-1.89(116)
17	+0.572(72)	+0.138(84)	-1.565(82)	
18	+0.660(88)	+0.306(264)	-1.532(164)	

^a Measured in dichloromethane with 0.1 M Bu₄NPF₆ as the electrolyte and a Pt disk working electrode at a scan rate of 110 mV s⁻¹.

713 nm. The photophysical profiles of zinc derivatives **17** and **18** as well as *seco*-porphyrazine **19** were determined. Previously, it has been suggested that because of the minimal fluorescence or intersystem crossing observed for porphyrazine **14** the dominant deactivation pathway for the first excited singlet state is internal conversion to the ground state followed by vibrational relaxation.²⁷ The vibrational relaxation is aided by the strong coupling of the nonbonding electron pairs of the peripheral nitrogen atoms to the macrocyclic core. Conversion of **14** to the corresponding *seco*-porphyrazine, however, results in decoupling of the lone-pair electrons from the ring, and the subsequent macrocycle displays high quantum yields for both intersystem crossing ($\Phi_T = 0.64$) and quenching ($\Phi_\Delta = 0.54$).²⁷ The high quantum yield of triplet-state formation is also attributed to the amido carbonyl groups, which are known to promote intersystem crossing.²⁸ Decoupling of the lone-pair electrons by the acetyl or trifluoroacetyl groups in **17** and **18** should also hinder vibrational relaxation, therefore promoting intersystem crossing aided by the carbonyl groups. Indeed, macrocycles **17** and **18** display singlet-oxygen quantum yields of 0.30 and 0.69, respectively. This reinforces the assumption that decoupling of the nitrogen lone pairs from the ring system facilitates intersystem crossing. Alternatively, the conformation of the amido functionality could provide a steric barrier, preventing the lone-pair electrons on the neighboring amino group from fully

SCHEME 4



Reagents and conditions:

- (a) MeOH, cat. TFA, 20 °C, 2 h, 90 %;
 (b) NaBH₄, MeOH, THF, 20 °C, 2 h, 99 %;
 (c) Me₂SO₄, NaH, THF, -30 to 20 °C, 18 h, 76 %.

conjugating with the ring system. Also, *seco*-porphyrazine **19** exhibits a singlet-oxygen quantum yield of 0.87, which is the highest value recorded for the *seco*-porphyrazines so far.²⁹ Presumably, the newly formed imido functionality efficiently aids intersystem crossing. In addition, the fluorescence quantum yields for porphyrazines **17**, **18**, and **19** are 0.01, 0.07, and 0.02, respectively, with corresponding lifetimes of 0.91, 2.40, and 0.70 ns. Therefore, for these macrocycles, relaxation via fluorescence is only a minor deactivation pathway.

In an attempt to extend this methodology, doubly tagged maleonitrile **22** was prepared in three steps from aldehyde **2** and dinitrile **4**. Condensation of aldehyde **2** and amine **4** in methanol with TFA catalysis gave imine **20**, which was subsequently reduced with sodium borohydride to give doubly tagged maleonitrile **21** in 89% yield in two steps. This was used without further purification. Methylation of dinitrile **21**, as before, gave doubly tagged dinitrile **22** in good yield (Scheme 4).

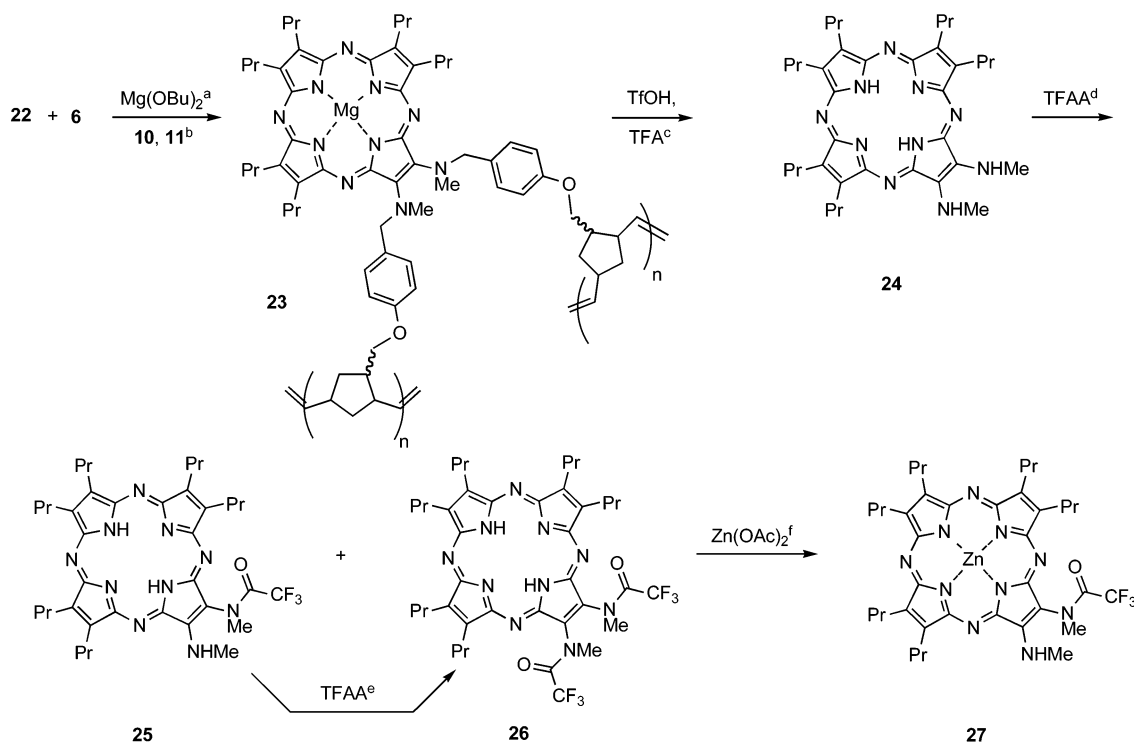
Crossover macrocyclization of aminomaleonitrile **22** and dipropylmaleonitrile **6** and ROM polymerization using catalyst **10** and cross-linker **11** gave heavily cross-linked ROM polymer **23** as a blue solid (Scheme 5). Treatment of polymer **23** with 10% TFA in dichloromethane failed to release any significant amount of porphyrazine products, whereas only decomposition was observed at higher concentrations of TFA. In contrast, polymer **23** was allowed to stand in dichloromethane containing 1 M triflic acid and 2 M TFA for 1 h at room

(27) Montalban, A. G.; Meunier, H. G.; Ostler, R. B.; Barrett, A. G. M.; Hoffman, B. M.; Rumbles, G. *J. Phys. Chem.* **1999**, *103*, 4352.

(28) Gilbert, G.; Baggott, J. *Essentials of Molecular Photochemistry*; Blackwell: Cambridge, MA, 1991; p 126.

(29) Montalban, A. G.; Baum, S.; Hoffman, B. M.; Barrett, A. G. M. *J. Chem. Soc., Dalton Trans.* **2003**, 2093.

SCHEME 5



Reagents and conditions:

- (a) $\text{Mg}(\text{O}^i\text{Bu})_2$, $^i\text{BuOH}$, Δ , 24 h; (b) 1 mol % **10**, **11**, CH_2Cl_2 , 40°C 18 h; (c) CH_2Cl_2 , 1 M TfOH , 2 M TFA , 20°C , 1 h; (d) TFAA , pyridine, 0°C , 10 mins; (e) TFAA , pyridine, 0°C , 1 h, 5%; (f) $\text{Zn}(\text{OAc})_2$, DMF , 80°C , 16 h, 72%.

temperature (Scheme 5) to release the unstable and easily oxidized porphyrazine **24**, which was used immediately for further transformations. Interestingly, the presence of triflic acid resulted in the standard purple porphyrazine color being replaced by brown for the duration of the cleavage, presumably due to protonation of the meso nitrogen atoms and disrupted aromaticity.

Unfortunately, functionalization of porphyrazine **24** was also problematic, and attempts to prepare acetamide derivatives were unsuccessful. Crude porphyrazine **24** was allowed to react with trifluoroacetic anhydride in degassed pyridine at 0°C to give a mixture of mono- and diamido porphyrazines **25** and **26**, which were separated by chromatography. Monoamide **25** was reacylated to yield additional diamido porphyrazine **26**, which could be isolated by filtration through silica in 5% yield in five steps from maleonitrile **22** and with >99% purity as judged by HPLC (Scheme 5). Porphyrazine **26** also displayed broadening of the NMR spectra in deuterated chloroform but displayed a clear NMR spectrum in pyridine- d_5 . Reaction of porphyrazine **26** with zinc acetate in DMF at 80°C gave zinc derivative **27**, which resulted from concomitant metalation and partial deacylation.

The electronic absorption spectra for free-base **26** and novel zinc derivative **27** are shown in Figure 4. The spectra resemble the previously encountered spectra for A_3B porphyrazines **13** and **14** (Figure 1). The broadening effect of the nitrogen nonbonding electrons (vide supra) is no longer apparent, and both **26** and **27** display sharpened, well-defined spectra. This has been observed previously on decoupling of the nitrogen lone pairs from the ring system following oxidation²⁹ or peripheral meta-

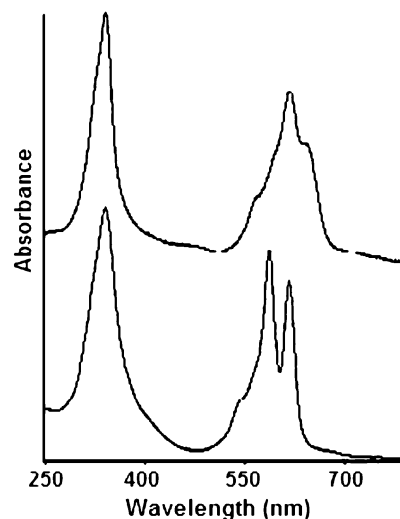


FIGURE 4. UV-vis spectra for porphyrazines **26** and **27** in CH_2Cl_2 .

lation.^{24,30} Immediately, this suggests that the electronically deactivating trifluoroacetyl groups prevent coupling of the nitrogen lone-pair electrons to the macrocyclic ring. Porphyrazine **26** exhibits a red-shifted, split Q band with Q_x and Q_y absorbances at 585 and 616 nm. The splitting can be assigned to the reduced symmetry of the free-base macrocycle. Zinc derivative **27** displays a broadened Q band centered around 617 nm with ad-

(30) Goldberg, D. P.; Michel, S. L.; White, A. J. P.; Williams, D. J.; Barrett, A. G. M.; Hoffman, B. M. *Inorg. Chem.* **1998**, *37*, 2100.

TABLE 2. Electrochemical Study of Porphyrazines **26** and **27**

	comparison of half-wave potentials (V vs Fc ⁺ /Fc) ^a , E _{1/2} (ΔE _p , mV)			
	pz ²⁺ /pz ⁺	pz ⁺ /pz	pz/pz ¹⁻	pz ¹⁻ /pz ²⁻
26		+0.838(122)	-1.184(102)	-1.591(120)
27	+0.737(148)	+0.237(72)	-1.526(164)	

^a Measured in dichloromethane with 0.1 M Bu₄NPF₆ as the electrolyte and a Pt disk working electrode at a scan rate of 110 mV s⁻¹.

ditional shoulders at 572 and 644 nm. The emission spectrum of porphyrazine **27** (λ_{ex} = 346 nm) displays a maxima at 659 nm.

Substitution of two electronically deactivating trifluoroacetyl groups onto the peripheral amino groups should result in complete decoupling of the nonbonding electrons, leading to an increase in the oxidation potential of the resulting porphyrazines. Consequently, the first oxidation potential of porphyrazine **26** is +0.838 V, indicating that the macrocycle is 968 mV more difficult to oxidize than free base **13** (Table 2). Impressively, this compound is more difficult to oxidize than the octapropyl- and octamethylthioporphyrazines, which display a reversible oxidation in the +0.65–0.70 V region.⁴ Free-base porphyrazine **26** also exhibits two reversible ring-based reductions at -1.18 and -1.59 V. (Table 2). Alternatively, novel zinc derivative **27** displays vastly different redox potentials than free-base **26**. The first oxidation potential of **27** is +0.237 V; it is 69 mV easier to oxidize than the related monotrifluoroacetylated porphyrazine **18**. In general, the redox potentials for **27** mirror those of the monoacetylated macrocycles (see Table 1).

The photophysical profile of zinc derivative **27** was determined. As previously stated, decoupling of the lone-pair electrons by the trifluoroacetyl groups hinders vibrational relaxation, therefore promoting intersystem crossing aided by the carbonyl groups (vide supra). Curiously, macrocycle **27** displays an impressive singlet-oxygen quantum yield of 0.88. This superb result is comparable to *seco*-porphyrazine **19**, and porphyrazine **27** therefore shows the highest photosensitizing ability of any of the porphyrazine macrocycles reported to date. The reason that novel derivative **27** has an increasing sensitizing ability relative to monotrifluoroacetylated porphyrazine **17** is yet to be established, and further studies are underway. Porphyrazine **27** showed a fluorescence quantum yield of 0.10 with a corresponding lifetime of 2.70 ns.

Conclusions

The development and application of a new ROM polymerization–release strategy for the selective synthesis of novel A₃B amino porphyrazines has been described. Acetyl or trifluoroacetyl substitution of the peripheral amino groups resulted in profound differences in the electronic structure of each macrocycle. All of the amido-functionalized porphyrazines showed increased oxidation potentials compared to the corresponding dialkylamino-substituted porphyrazines as a result of the reduced electron donation into the macrocycle by the nitrogen-centered substituents. Additionally, the relationship between the coupling of the nitrogen nonbonding

electrons with the ring system and the efficiency of sensitization to produce singlet oxygen has been confirmed. Furthermore, novel trifluoroacetylated porphyrazine **27** exhibits an excellent singlet-oxygen quantum yield (Φ_Δ = 0.88) and is the most potent porphyrazine sensitizer synthesized to date. The synthetic flexibility of this novel methodology for the synthesis of other porphyrazine derivatives will be the subject of future reports.

Experimental Section

4-(Bicyclo[2.2.1]hept-5-en-2-ylmethoxy)benzaldehyde (2). 4-Hydroxybenzaldehyde (1.32 g, 10.8 mmol) was added to tosylate **1**²¹ (3.0 g, 10.8 mmol) and Cs₂CO₃ (5.27 g, 16.2 mmol) in DMF (20 mL) under N₂. The mixture was heated to 100 °C for 16 h, poured into H₂O (50 mL), and extracted with Et₂O (3 × 50 mL). The combined organic extracts were washed with saturated aqueous NH₄Cl (3 × 50 mL), dried (MgSO₄), filtered, and rotary evaporated. Chromatography (SiO₂, hexanes/EtOAc, 9:1) gave aldehyde **2** (2.37 g, 96%) as a colorless oil containing a mixture of isomers. *R*_f: 0.33 (hexanes/EtOAc, 9:1); IR (neat): 1692, 1640, 1510, 1256, 1159, 1015 cm⁻¹; ¹H NMR (300 MHz, CDCl₃, δ): 0.64 (*app-d*, *J* = 10.0 Hz, 1H), 1.35 (m, 1H), 1.50 (m, 1H), 1.95 (m, 1H), 2.59 (br m, 1H), 2.88 (br m, 1H), 3.06 (br m, 1H), 3.65 (t, *J* = 9.0 Hz, 1H), 3.80 (m, 1H), 5.97 (br m, 1H), 6.20 (m, 1H), 6.99 (d, *J* = 9.0 Hz, 2H), 7.82 (d, *J* = 9.0 Hz, 2H), 9.89 (s, 1H); ¹³C NMR (75 MHz, CDCl₃, δ): 29.0, 38.5, 42.3, 43.9, 49.5, 71.9, 114.8, 129.7, 132.0, 132.2, 137.8, 164.3, 190.9; MS (CI) *m/z*: 229 [M + H]⁺; HRMS (CI): [M + H]⁺ calcd for C₁₅H₁₇O₂, 229.1229; found, 229.1224. Anal. Calcd for C₁₅H₁₆O₂: C, 78.92; H, 7.06. Found: C, 79.00; H, 7.00.

2-Amino-3-[(4-(bicyclo[2.2.1]hept-5-en-2-ylmethoxy)-benzylidene)amino]but-2-enedinitrile (3). Diaminomaleonitrile (1.04 g, 9.6 mmol) and aldehyde **2** (2.20 g, 9.6 mmol) in EtOH (10 mL) were heated to reflux overnight. The yellow solid, which precipitated out of the solution, was filtered off and washed with cold EtOH (5 mL). The filtrate was heated to reflux for another 4 h, and the precipitated solid was filtered, washed, and combined with the previous crop. This gave imine **3** (2.25 g, 73%) as a yellow solid containing a mixture of isomers, which was used without further purification: mp 207–209 °C; IR (neat): 3411, 3297, 2245, 2205, 1606, 1249, 826 cm⁻¹; ¹H NMR (300 MHz, DMSO-*d*₆, δ): 0.64 (*app-d*, *J* = 10.0 Hz, 1H), 1.31 (m, 1H), 1.50 (m, 1H), 1.95 (m, 1H), 2.50 (m, 1H, obscured by DMSO), 2.88 (br m, 1H), 3.06 (br m, 1H), 3.64 (t, *J* = 9.0 Hz, 1H), 3.77 (m, 1H), 5.98 (br m, 1H), 6.21 (m, 1H), 6.99 (d, *J* = 8.0 Hz, 2H), 7.76 (br s, 2H), 7.99 (d, *J* = 8.0 Hz, 2H), 8.20 (s, 1H); ¹³C NMR (125 MHz, DMSO-*d*₆, δ): 28.7, 37.8, 41.7, 43.4, 49.0, 71.4, 103.1, 113.9, 114.6, 114.7, 125.9, 128.3, 131.0, 132.2, 137.5, 154.7, 161.6; MS (CI) *m/z*: 319 [M + H]⁺; HRMS (CI): [M + H]⁺ calcd for C₁₉H₁₉N₄O, 319.1559; found, 319.1565.

2-Amino-3-[4-(bicyclo[2.2.1]hept-5-en-2-ylmethoxy)benzylamino]but-2-enedinitrile (4). NaBH₄ (0.36 g, 9.5 mmol) was added in portions to a suspension of imine **3** (1.01 g, 3.17 mmol) in dry THF (15 mL) and MeOH (10 mL) under N₂. The slurry was stirred for 2 h, during which the mixture turned homogeneous. The solution was poured into ice/H₂O (150 mL), the resultant cream solid was filtered off, and the residual H₂O was removed by azeotrope with PhMe (2 × 30 mL). This gave amine **4** (0.97 g, 96%) as a brown solid containing a mixture of isomers, which was used without further purification: mp 163–165 °C; IR (neat): 3329, 2218, 2204, 1618, 1510, 1379, 1238 cm⁻¹; ¹H NMR (300 MHz, DMSO-*d*₆, δ): 0.59 (*app-d*, *J* = 11.0 Hz, 1H), 1.29 (m, 2H), 1.87 (m, 1H), 2.50 (m, 1H, obscured by DMSO), 2.86 (br m, 1H), 2.96 (br m, 1H), 3.51 (t, *J* = 9.0 Hz, 1H), 3.67 (m, 1H), 4.14 (d, *J* = 5.0 Hz, 2H), 5.62 (br m, 3H), 5.95 (m, 1H), 6.19 (m, 1H), 6.89 (d, *J* = 8.0 Hz, 2H), 7.18 (d, *J* = 8.0 Hz, 2H); ¹³C NMR (125 MHz, DMSO-*d*₆,

δ): 28.7, 37.8, 41.7, 43.4, 48.4, 48.9, 71.0, 107.6, 108.2, 114.4, 115.8, 116.7, 128.6, 130.9, 132.1, 137.3, 157.9; MS (CI) m/z : 338 [M + NH₄]⁺; HRMS (CI): [M + NH₄]⁺ calcd for C₁₉H₂₄N₅O, 338.1981; found, 338.1986.

2-[(4-(Bicyclo[2.2.1]hept-5-en-2-ylmethoxy)benzyl)methylamino]-3-(dimethylamino)-but-2-enedinitrile (5). Dinitrile **4** (0.86 g, 2.7 mmol) in dry THF (10 mL) was added to NaH (0.54 g, 13.5 mmol, 60% suspension in mineral oil) in dry THF (20 mL) at -30 °C under N₂. The mixture was allowed to warm to -10 °C, and dimethyl sulfate (1.28 mL, 13.5 mmol) was added over 30 min, after which the mixture was allowed to warm to 20 °C and stirred for 18 h. After rotary evaporation, aqueous 2 M NaOH (50 mL) was added, and the suspension was stirred for 1 h to remove residual dimethyl sulfate followed by the addition of Et₂O (50 mL). The layers were separated, and the aqueous layer was washed with Et₂O (50 mL). The combined organic extracts were washed with H₂O (30 mL), dried (MgSO₄), filtered, and rotary evaporated. Chromatography (SiO₂, hexanes/EtOAc, 7:3) gave dinitrile **5** (0.91 g, 93%) as a viscous yellow oil containing a mixture of isomers. R_f : 0.55 (hexanes/EtOAc, 7:3); IR (neat): 2183, 1596, 1512, 1245, 1026 cm⁻¹; ¹H NMR (400 MHz, CDCl₃, δ): 0.63 (m, 1H), 1.32 (*app-d*, $J = 11.8$ Hz, 1H), 1.47 (m, 1H), 1.91 (m, 1H), 2.54 (m, 1H), 2.68 (s, 3H), 2.78 (s, 6H), 2.84 (m, 1H), 3.03 (m, 1H), 3.54 (t, $J = 9.1$ Hz, 1H), 3.69 (m, 1H), 4.05 (s, 2H), 5.97 (m, 1H), 6.17 (m, 1H), 6.84 (d, $J = 11.5$ Hz, 2H), 7.13 (d, $J = 11.5$ Hz, 2H); ¹³C NMR (125 MHz, CDCl₃, δ): 29.1, 38.4, 40.2, 42.1, 42.2, 43.9, 49.4, 57.9, 71.6, 114.3, 114.6, 114.8, 114.9, 120.4, 128.4, 129.9, 132.3, 137.6, 158.9; MS (CI) m/z : 363 [M + H]⁺; HRMS (CI): [M + H]⁺ calcd for C₂₂H₂₇N₄O, 363.2185; found, 363.2189. Anal. Calcd for C₂₂H₂₆N₄O: C, 72.90; H, 7.23; N, 15.46. Found: C, 73.20; H, 7.20; N, 15.26.

7,8,12,13,17,18-Hexapropyl-2-(dimethylamino)-3-(methylamino)porphyrazine (12). Mg (0.22 g, 9.0 mmol), I₂ (2 crystals), and 1-butanol (20 mL) were heated to reflux for 24 h under N₂. The mixture was allowed to cool when dinitrile **5** (0.22 g, 0.6 mmol) and dipropylmaleonitrile **6**²³ (0.97 g, 5.96 mmol) in 1-butanol (10 mL) were added and the mixture was heated to reflux for another 24 h. The solvent was evaporated under reduced pressure and formed an azeotrope with PhMe (2 × 50 mL). The residue was preabsorbed onto silica, and the solids were extracted with hexanes/EtOAc (8:2) until the intensity of the initial blue color had decreased and elution of a purple pigment had begun. The combined extracts were rotary evaporated, and the residue was dissolved in degassed CH₂Cl₂ (2 mL) under N₂. Cross-linker **11** (15.3 mg, 0.07 mmol) in CH₂Cl₂ (0.5 mL) was added followed by catalyst **10** (5.0 mg, 6.0 μ mol), and the mixture was heated to 40 °C for 12 h. CH₂Cl₂ (2 mL), MeCN (1 mL), and ethyl vinyl ether (1 mL) were added, and the mixture was heated to 40 °C for 1 h. The gel was filtered and washed sequentially with CH₂Cl₂ (3 × 20 mL) and further extracted with CH₂Cl₂ (Soxhlet) for 12 h. This left the insoluble ROM polymer (**9**, 0.11 g) as a blue solid. A degassed solution of 10% trifluoroacetic acid in CH₂Cl₂ (5 mL) was added to a suspension of ROM polymer **9** (0.11 g) under Ar, and the suspension was shaken for 1 h. The resulting mixture was filtered into H₂O (20 mL), and the resulting layers were separated. The organic layer was washed with saturated aqueous NaHCO₃ (30 mL), dried (MgSO₄), filtered, and rotary evaporated. The solution of the cleavage product was filtered through silica with further extraction (hexanes/EtOAc, 9:1) to give diamine **12** (61 mg, 16%) as an unstable purple solid, which was used immediately. R_f : 0.80 (hexanes/EtOAc, 1:1.5); UV-vis (hexanes/EtOAc, 9:1) λ_{\max} 338, 549, 595, 625, 652 nm; MS (FAB) m/z : 638 [M⁺]; HRMS (FAB): [M⁺] calcd for C₃₇H₅₄O₁₀, 638.4533; found, 638.4502.

7,8,12,13,17,18-Hexapropyl-2-(dimethylamino)-3-(N-methylacetamido)porphyrazine (15). Ac₂O (0.05 mL, 0.53 mmol) was added to porphyrazine **12** (7.5 mg, 0.012 mmol) in degassed pyridine (2 mL) under N₂, and the mixture was heated at reflux for 18 h. The mixture was allowed to cool, ScavengePore phenethyl piperidine (0.7–1.5 mmol/g) (1 g) was

added, and the resulting suspension was heated at reflux for 1 h. After rotary evaporation, Et₂O (20 mL) was added to the residue, the mixture was filtered, and the filtrate was evaporated under reduced pressure. The product in hexanes/EtOAc (7:3) was filtered through silica to give amide **15** as a purple/blue solid (7.6 mg, 95%). R_f : 0.23 (hexanes/EtOAc, 6:4); HPLC: $P_{\text{HPLC}} = 100\%$, $t_R = 16.5$ min; IR (neat): 3311, 1669, 1603, 1463, 1146 cm⁻¹; UV-vis (CH₂Cl₂) λ_{\max} (log ϵ) 342 (4.08), 549 (3.50), 591 (3.61), 617 (3.59), 668 (3.56) nm; ¹H NMR (500 MHz, CDCl₃, δ): -1.60 (br s, 2H), 1.20 (t, $J = 3$ Hz, 3H), 1.25 (m, 15H), 2.19 (s, 3H), 2.31 (m, 12H), 3.78 (m, 7H), 3.92 (m, 8H), 4.14 (s, 6H); ¹³C NMR (125 MHz, CDCl₃, δ): 14.5, 14.7, 14.8, 22.9, 25.3, 25.4, 25.5, 27.7, 28.0, 28.1, 28.2, 29.7, 39.2, 43.2, 117.7, 139.8, 141.2, 142.2, 142.6, 144.3, 144.9, 145.0, 145.2, 148.1, 148.5, 153.3, 159.4, 160.5, 162.6, 174.0; MS (FAB) m/z : 681 [M⁺]; HRMS (FAB): [M⁺] calcd for C₃₉H₅₆N₁₀O, 680.4639; found, 680.4643.

7,8,12,13,17,18-Hexapropyl-2-(dimethylamino)-3-(N-methyltrifluoroacetamido)porphyrazine (16). Trifluoroacetic anhydride (0.2 mL, 1.4 mmol) was added to porphyrazine **12** (8 mg, 0.013 mmol) in degassed pyridine (2 mL) at 0 °C under Ar, and the mixture was stirred for 1 h at 0 °C. The mixture was allowed to warm to 20 °C, ScavengePore phenethyl piperidine (0.7–1.5 mmol/g) (1 g) was added, and then the resulting suspension was stirred at 20 °C for 1 h. After rotary evaporation, the residue was extracted with Et₂O (20 mL) and filtered, and then the filtrate was washed with H₂O (30 mL), saturated aqueous NaHCO₃ solution (30 mL), saturated aqueous NH₄Cl solution (30 mL), and brine (30 mL). The organic layer was dried (MgSO₄), filtered, and rotary evaporated. The product in hexanes/EtOAc (95:5) was filtered through silica to give amide **16** (6.2 mg, 65%) as a blue solid. R_f : 0.43 (hexanes/EtOAc, 8:2); HPLC: $P_{\text{HPLC}} = 93\%$, $t_R = 8.7$ min; IR (neat): 1704, 1607, 1463, 1381, 1199, 1154 cm⁻¹; UV-vis (CH₂Cl₂) λ_{\max} (log ϵ) 344 (4.35), 540 (3.65), 595 (3.93), 670 (3.83) nm; ¹H NMR (500 MHz, CDCl₃, δ): -1.61 (br s, 2H), 1.16–1.33 (m, 18H), 2.30 (m, 12H), 3.76 (m, 4H), 3.93 (m, 11H), 4.14 (s, 6H); ¹³C NMR (125 MHz, CDCl₃, δ): 14.5, 14.7, 25.2, 25.3, 25.4, 25.5, 27.7, 28.0, 28.1, 28.2, 29.7, 41.6, 43.2, 112.6, 115.7, 118.2, 139.6, 141.0, 142.0, 142.4, 144.0, 144.4, 144.6, 145.3, 145.3, 147.4, 149.5, 153.4, 159.9, 160.1, 161.4, 163.6; MS (FAB) m/z : 735 [M⁺]; HRMS (FAB): [M⁺] calcd for C₃₉H₅₃F₃N₁₀O, 734.4356; found, 734.4371.

7,8,12,13,17,18-Hexapropyl-2-(dimethylamino)-3-(N-methylacetamido)porphyrazinato]zinc(II) (17). A mixture of porphyrazine **15** (2.2 mg, 0.003 mmol) and Zn(OAc)₂·2H₂O (1 mg, 0.005 mmol) in dry DMF (2 mL) was heated to 80 °C for 16 h under N₂. Rotary evaporation and chromatography (SiO₂, hexanes/EtOAc, 1:1) gave porphyrazine **17** (2.0 mg, 83%) as a turquoise solid. R_f : 0.47 (hexanes/EtOAc, 1:1); IR (neat): 1674, 1603, 1463, 1148, 1082 cm⁻¹; UV-vis (CH₂Cl₂) λ_{\max} (log ϵ) 342 (4.55), 508 (3.73), 626 (4.25) nm; ¹H NMR (500 MHz, pyridine-*d*₅, δ): 1.28–1.39 (m, 18H), 2.35 (s, 3H), 2.48 (m, 12H), 3.94–4.12 (m, 21H); ¹³C NMR (125 MHz, pyridine-*d*₅, δ): 14.8, 15.0, 23.1, 25.9, 26.0, 28.4, 28.7, 39.2, 42.8, 106.4, 118.2, 142.5, 143.2, 143.6, 144.0, 144.2, 144.9, 148.6, 151.2, 156.7, 157.0, 158.9, 159.5, 160.4, 173.2; MS (FAB) m/z : 744 [M⁺]; HRMS (FAB): [M⁺] calcd for C₃₉H₅₄N₁₀OZn, 742.3773; found, 742.3768.

7,8,12,13,17,18-Hexapropyl-2-(dimethylamino)-3-(methyltrifluoroacetamido)porphyrazinato]zinc(II) (18). Porphyrazine **16** (6.0 mg, 0.0082 mmol), Zn(OAc)₂·2H₂O (2.5 mg, 0.011 mmol), and dry DMF (2 mL) were heated to 80 °C for 16 h under N₂. The solvent was rotary evaporated, and the product was chromatographed (SiO₂, hexanes/EtOAc, 7.5:2.5) to give porphyrazine **18** (5.0 mg, 76%) as a turquoise solid. R_f : 0.79 (hexanes/EtOAc, 7:3); IR (neat): 1703, 1678, 1597, 1462, 1210, 1152 cm⁻¹; UV-vis (CH₂Cl₂) λ_{\max} (log ϵ) 342 (4.20), 490 (3.26), 630 (3.94) nm; ¹H NMR (500 MHz, pyridine-*d*₅, δ): 1.29–1.38 (m, 18H), 2.44 (m, 12H), 3.91–4.14 (m, 21H); ¹³C NMR (125 MHz, pyridine-*d*₅, δ): 14.8, 15.0, 25.8, 26.0, 28.3, 28.6, 41.9, 42.9, 112.6, 142.5, 143.2, 143.6, 144.2, 145.0, 156.8,

157.0, 159.1, 159.6, 160.5; MS (FAB) m/z : 796 [M⁺]; HRMS (FAB): [M⁺] calcd for C₃₉H₅₁F₃N₁₀OZn, 796.3491; found, 796.3528.

[7,8,12,13,17,18-Hexapropyl-2-(dimethylamino)-3-(methylacetamido)-2-*seco*-2,3-dioxoporphyrazinato]zinc(II) (19). Porphyrazine **17** (2.0 mg, 2.7 μmol) in CH₂Cl₂ (40 mL) was stirred in air for 3 days. Rotary evaporation and chromatography (SiO₂, hexanes/EtOAc, 1:1) gave *seco*-porphyrazine **19** (1.1 mg) and unreacted porphyrazine **17** (0.9 mg). Recovered porphyrazine **17** was resubjected to the reaction conditions for another 5 days, and then the solution was rotary evaporated and chromatographed (SiO₂, hexanes/EtOAc, 1:1). In total, this gave *seco*-porphyrazine **19** (1.8 mg, 86%) as a magenta solid. R_f : 0.61 (hexanes/EtOAc, 1:1); IR (neat): 1706, 1673, 1600, 1492, 1461, 1259, 1081 cm⁻¹; UV-vis (CH₂Cl₂) λ_{max} (log ε) 341 (4.10), 357 (4.09), 572 (3.86), 651 (3.98) nm; ¹H NMR (500 MHz, pyridine-*d*₅, δ): 0.89 (m, 6H), 1.17–1.50 (m, 22H), 1.71 (m, 2H), 2.21 (m, 1H), 2.46 (m, 3H), 2.81 (s, 3H), 3.45 (s, 3H), 3.77 (m, 1H), 3.97 (m, 6H), 4.20 (s, 3H), 3.39 (m, 4H); ¹³C NMR (125 MHz, pyridine-*d*₅, δ): 11.1, 14.2, 14.8, 15.0, 23.2, 24.1, 25.8, 26.0, 27.3, 28.0, 28.5, 28.6, 29.2, 30.0, 30.7, 34.0, 35.2, 39.1, 39.5, 68.3, 129.3, 131.5, 133.2, 141.7, 142.1, 143.0, 143.2, 145.1, 145.3, 152.3, 155.1, 156.0, 156.7, 157.0, 157.3, 167.9, 169.7, 171.2, 174.4; MS (FAB) m/z : 774 [M⁺]; HRMS (FAB): [M+H] calcd for C₃₉H₅₅N₁₀O₂Zn, 775.3750; found, 775.3778.

2-[4-(Bicyclo[2.2.1]hept-5-en-2-ylmethoxy)benzylamino]-3-[(4-(bicyclo[2.2.1]hept-5-en-2-ylmethoxy)benzylidene)amino]but-2-enedinitrile (20). TFA (2 drops) was added to amine **4** (1.71 g, 5.3 mmol) and aldehyde **2** (1.27 g, 5.3 mmol) in MeOH (10 mL). After 2 h, the yellow precipitate was filtered off and washed with Et₂O (10 mL) to give imine **20** (2.53 g, 90%) as a yellow solid containing a mixture of isomers, which was insoluble in most organic solvents and was used without further purification: mp 177–179 °C; IR (neat): 2229, 2199, 1602, 1512, 1250, 1165 cm⁻¹; ¹H NMR (500 MHz, DMSO-*d*₆, δ): 0.58 (m, 2H), 1.24 (m, 2H), 1.37 (m, 2H), 1.87 (m, 2H), 2.50 (m, 2H, obscured by DMSO), 2.80 (m, 2H), 2.94 (m, 2H), 3.50 (t, $J = 9.0$ Hz, 1H), 3.59 (t, $J = 9.0$ Hz, 1H), 3.65 (m, 1H), 3.75 (m, 1H), 4.48 (d, $J = 6.4$ Hz, 2H), 5.93 (m, 2H), 6.17 (m, 2H), 6.90 (d, $J = 9.0$ Hz, 2H), 6.98 (d, $J = 9.0$ Hz, 2H), 7.23 (d, $J = 9.0$ Hz, 2H), 7.95 (d, $J = 9.0$ Hz, 2H), 8.20 (m, 1H), 8.43 (m, 1H); ¹³C NMR (125 MHz, DMSO-*d*₆, δ): 28.6, 38.1, 41.6, 43.4, 48.4, 48.9, 71.1, 71.3, 103.6, 113.3, 113.7, 114.6, 114.7, 127.0, 128.1, 128.4, 130.4, 131.0, 132.1, 137.4, 155.0, 158.1, 161.7; MS (FAB) m/z : 531 [M⁺]; HRMS (FAB): [M⁺] calcd for C₃₄H₃₄N₄O₂, 530.2682; found, 530.2678.

2,3-Bis-[4-(bicyclo[2.2.1]hept-5-en-2-ylmethoxy)benzylamino]but-2-enedinitrile (21). NaBH₄ (0.47 g, 12.4 mmol) was added in portions to a suspension of imine **20** (2.2 g, 4.15 mmol) in dry THF (23 mL) and MeOH (15 mL) under N₂. The slurry was stirred for 2 h and poured into ice/H₂O (150 mL), and then the sticky residue was filtered, redissolved in THF (30 mL), and washed through the filter with additional THF. After rotary evaporation, residual H₂O was removed by azeotrope with PhMe (2 × 30 mL) to leave diamine **21** (2.18 g, 99%) as a brown oil containing a mixture of isomers, which was used without further purification. IR (neat): 2203, 1607, 1512, 1247, 1175 cm⁻¹; ¹H NMR (500 MHz, DMSO-*d*₆, δ): 0.58 (m, 2H), 1.24 (m, 2H), 1.37 (m, 2H), 1.87 (m, 2H), 2.50 (m, 2H, obscured by DMSO), 2.80 (br s, 2H), 2.95 (br s, 2H), 3.49 (t, $J = 9.0$ Hz, 2H), 3.65 (m, 2H), 4.15 (d, $J = 6.0$ Hz, 4H), 4.48 (m, 2H), 5.94 (m, 2H), 6.18 (m, 2H), 6.85 (d, $J = 8.6$ Hz, 4H), 7.12 (d, $J = 8.6$ Hz, 4H); ¹³C NMR (125 MHz, DMSO-*d*₆, δ): 28.7, 37.8, 41.7, 43.4, 48.4, 48.9, 71.0, 109.8, 114.4, 115.4, 128.7, 131.0, 132.1, 137.3, 158.0; MS (FAB) m/z : 533 [M⁺]; HRMS (FAB): [M–H]⁺ calcd for C₃₄H₃₅N₄O₂, 531.2760; found, 531.2763.

2,3-Bis-[4-(bicyclo[2.2.1]hept-5-en-2-ylmethoxy)benzylmethylamino]but-2-enedinitrile (22). Dinitrile **21** (2.1 g, 3.94 mmol) in dry THF (20 mL) was added to NaH (0.4 g, 9.85 mmol, 60% suspension in mineral oil) in dry THF (50 mL) at –30 °C under N₂. The mixture was allowed to warm to –10 °C, and dimethyl sulfate (0.82 mL, 8.67 mmol) was added over

30 min. The mixture was allowed to warm to 20 °C, stirred for 18 h, and rotary evaporated. NaOH (2 M, 50 mL) was added, and the suspension was stirred for 1 h to hydrolyze residual dimethyl sulfate. Et₂O (50 mL) was added, the layers were separated, and then the aqueous layer was washed with Et₂O (50 mL). The combined organic extracts were washed with H₂O (30 mL), dried (MgSO₄), filtered, and rotary evaporated. Chromatography (SiO₂, hexanes/EtOAc, 8:2) gave dinitrile **22** (1.67 g, 76%) as a viscous orange oil containing a mixture of isomers. R_f : 0.40 (hexanes/EtOAc, 8:2); IR (neat): 2184, 1597, 1512, 1247, 1175, 1023 cm⁻¹; ¹H NMR (500 MHz, CDCl₃, δ): 0.62 (m, 2H), 1.22–1.31 (m, 2H), 1.49 (m, 2H), 1.92 (m, 2H), 2.54 (m, 2H), 2.69 (s, 6H), 2.85 (m, 2H), 3.04 (m, 2H), 3.54 (t, $J = 9.2$ Hz, 2H), 3.69 (m, 2H), 4.11 (s, 4H), 5.96 (m, 2H), 6.18 (m, 2H), 6.82 (m, 4H), 7.05 (m, 4H); ¹³C NMR (125 MHz, CDCl₃, δ): 29.1, 38.4, 40.1, 42.2, 43.9, 49.4, 58.1, 71.6, 114.7, 114.9, 117.6, 127.9, 129.7, 132.3, 137.6, 158.9; MS (FAB) m/z : 561 [M⁺]; HRMS (FAB): [M⁺] calcd for C₃₆H₄₀N₄O₂, 560.3151; found, 560.3194.

7,8,12,13,17,18-Hexapropyl-2,3-bis(*N*-methyltrifluoroacetamido)porphyrazine (26). Mg (0.12 g, 5.1 mmol), I₂ (2 crystals), and 1-butanol (20 mL) were heated to reflux for 24 h under N₂. The mixture was allowed to cool, dinitrile **22** (0.19 g, 0.34 mmol) and dipropylmaleonitrile **6**²³ (0.55 g, 3.40 mmol) in 1-butanol (10 mL) were added, and then the mixture was heated to reflux for another 24 h. The solvent was removed by rotary evaporation and subsequent azeotrope with PhMe (2 × 50 mL). The residue was preabsorbed onto silica and added to additional silica, which was washed extensively with hexanes/EtOAc (8:2) until the intensity of the initial blue color had decreased and elution of a purple pigment had begun. After rotary evaporation, the residue was dissolved in degassed CH₂Cl₂ (2 mL) under N₂, cross-linker **11** (10.0 mg, 0.038 mmol) in CH₂Cl₂ (0.5 mL) was added followed by catalyst **10** (3.0 mg, 3.4 μmol), and then the mixture was heated to 40 °C for 12 h. CH₂Cl₂ (2 mL), MeCN (1 mL), and ethyl vinyl ether (1 mL) were added, and the mixture was further heated to 40 °C for 1 h. The gel was filtered off and washed sequentially with CH₂Cl₂ (3 × 20 mL) and further extracted with CH₂Cl₂ (Soxhlet) for 12 h to leave the insoluble ROM polymer (**23**, 70 mg) as a blue solid. Degassed 1 M trifluoromethanesulfonic acid and 2 M trifluoroacetic acid in CH₂Cl₂ (3 mL) were added to a suspension of ROM polymer **23** (70 mg) under Ar, which was shaken at 20 °C for 1 h. The resulting mixture was filtered into H₂O (20 mL), and the resulting layers were separated. The organic layer was washed with saturated aqueous NaHCO₃ solution (30 mL), dried (MgSO₄), filtered, and rotary evaporated to give diamine **24** as a crude, unstable purple solid, which was used immediately. Trifluoroacetic anhydride (0.05 mL, 0.35 mmol) was added to porphyrazine **24** in degassed pyridine (2 mL) at 0 °C under Ar and stirred for 10 min at 0 °C. The mixture was poured into saturated aqueous NH₄Cl solution (20 mL) and extracted with EtOAc (30 mL). The organic layer was washed with saturated aqueous NH₄Cl solution (3 × 20 mL) to remove the pyridine and was dried (MgSO₄), filtered, and rotary evaporated. Chromatography (SiO₂, hexanes/EtOAc, 9:1) gave a mixture of monosubstituted porphyrazine **25** and disubstituted porphyrazine **26**. Porphyrazine **25**: (6.2 mg). R_f : 0.33 (hexanes/EtOAc, 9:1); IR (neat): 1697, 1650, 1463, 1193, 1144, 1086 cm⁻¹; UV-vis (CH₂Cl₂) λ_{max}: 344, 586, 680 nm; ¹H NMR (500 MHz, pyridine-*d*₅, δ): –1.15 (s, 2H), 1.01 (t, $J = 7.5$ Hz, 3H), 1.25–1.38 (m, 15H), 2.15 (sextet, $J = 7.5$ Hz, 2H), 2.41 (m, 10H), 3.68 (d, $J = 5.3$ Hz, 3H), 3.76 (t, $J = 7.5$ Hz, 2H) 3.88–4.01 (m, 10H), 4.10 (s, 3H), 9.48 (q, $J = 5.3$ Hz, 1H); ¹³C NMR (125 MHz, pyridine-*d*₅, δ): 14.5, 14.7, 15.0, 25.7, 25.8, 25.9, 27.5, 27.9, 28.3, 28.5, 30.0, 30.5, 41.5, 139.9, 141.9, 142.0, 142.7, 144.0, 144.9, 145.3, 145.7, 146.7, 147.0, 161.8, 163.9; MS (FAB) m/z : 720 [M⁺]; HRMS (FAB): [M⁺] calcd for C₃₈H₅₁F₃N₁₀O, 720.4199; found, 720.4199. Disubstituted porphyrazine **26** (7.3 mg): R_f : 0.78 (hexanes/EtOAc, 9:1); HPLC: $P_{\text{HPLC}} = 100\%$, $t_R = 7.1$ min; IR (neat): 1704, 1463, 1263, 1151, 1081 cm⁻¹; UV-vis (CH₂Cl₂)

λ_{\max} (log ϵ) 340 (4.16), 546 (3.55), 586 (4.08), 616 (4.01) nm; ^1H NMR (500 MHz, pyridine- d_5 , δ): -2.24 (s, 2H), 1.32–1.39 (m, 18H), 2.46 (m, 12H), 3.91–4.10 (m, 18H); ^{13}C NMR (125 MHz, pyridine- d_5 , δ): 14.9, 15.0, 25.8, 28.2, 28.5, 28.7, 39.9, 68.2, 116.3, 118.6, 129.3, 131.5, 142.7, 143.7, 145.6, 147.2, 148.1, 158.6, 166.8; MS (FAB) m/z : 817 [M^+]; HRMS (FAB): [M^+] calcd for $\text{C}_{40}\text{H}_{50}\text{F}_6\text{N}_{10}\text{O}_2$, 816.4022; found, 816.4016. Porphyrzine **25** (6.2 mg) was resubjected to the above reaction acylation conditions for 1 h at 0 °C. Following an analogous workup and filtration through silica (hexanes/EtOAc, 9:1), additional porphyrzine **26** (6.6 mg) was isolated. In total, this gave porphyrzine **26** (13.9 mg, 5%) as a violet solid.

[7,8,12,13,17,18-Hexapropyl-2-(methylamino)-3-(methyltrifluoroacetamido)porphyrzinato]-zinc(II) (27). Porphyrzine **26** (10.3 mg, 0.0126 mmol), $\text{Zn}(\text{OAc})_2 \cdot 2\text{H}_2\text{O}$ (3.9 mg, 0.018 mmol), and dry DMF (2 mL) were heated to 80 °C for 16 h under N_2 . Rotary evaporation and chromatography (SiO_2 , hexanes/EtOAc, 8:2) gave porphyrzine **27** (8.0 mg, 72%) as a turquoise solid. R_f : 0.35 (hexanes/EtOAc, 8:2); IR (neat): 1698, 1633, 1462, 1248, 1149, 1018 cm^{-1} ; UV-vis (CH_2Cl_2) λ_{\max} (log ϵ) 341 (4.62), 572 (4.05), 617 (4.46), 644 (4.29) nm; ^1H NMR (500 MHz, pyridine- d_5 , δ): 1.04 (t, $J = 7.3$ Hz, 3H), 1.24–1.37 (m, 15H), 2.22 (sextet, $J = 7.3$ Hz, 2H), 2.49 (m, 10H), 3.73 (d, $J = 5.3$ Hz, 3H), 3.80 (t, $J = 7.3$ Hz, 2H) 3.91–4.05 (m, 10H), 4.09 (s, 3H), 9.17 (q, $J = 5.3$ Hz, 1H); ^{13}C NMR (125 MHz, pyridine- d_5 , δ): 14.6, 14.8, 15.0, 25.7, 25.9, 26.0, 28.1, 28.3,

28.6, 30.7, 41.6, 142.3, 143.1, 143.8, 144.2, 144.9, 156.4, 156.6, 158.2, 158.6, 159.1, 160.7; MS (FAB) m/z : 784 [M^+]; HRMS (FAB): [M^+] calcd for $\text{C}_{38}\text{H}_{49}\text{F}_3\text{N}_{10}\text{OZn}$, 782.3334; found, 782.3309.

Acknowledgment. We thank Glaxo SmithKline for the generous endowment (to A.G.M.B.), the Royal Society and the Wolfson Foundation for a Royal Society Wolfson Research Merit Award (to A.G.M.B.), the Wolfson Foundation for establishing the Wolfson Centre for Organic Chemistry in Medical Sciences at Imperial College, the Engineering and Physical Sciences Research Council, the National Science Foundation, and Schering AG for generous support of our studies. We additionally thank Dr. Klaus Suhling and Miss Carolyn Jones for the loan of the equipment and assistance in the measurement of the fluorescence decays.

Supporting Information Available: General experimental procedures and structural data for all new compounds. This material is available free of charge via the Internet at <http://pubs.acs.org>.

JO047792Q